CNRS
Centre National de la Recherche Scientifique

INFN
Istituto Nazionale di Fisica Nucleare

Characterization and simulation of mirror surfaces

Massimo Galimberti

Laboratoire des Matériaux Avancés
7, avenue Pierre de Coubertin, 69622 Villeurbanne (FRANCE)

m.galimberti@lma.in2p3.fr

VIR-0038A-11
Issue: 1
Jan 25, 2011

VIRGO * A joint CNRS-INFN Project
Project Office: Traversa H di Via Macerata, I-56021 S.Stefano a Macerata (Pisa)
Secretariat: Telephone (+39) 050 752 511 * FAX (+39) 050 752 550 * e-mail W3@virgo.infn.it

Contents

Abstract

A method is presented to characterize the surface defects of Virgo mirrors via the power spectral density. The method is then applied to generate random surfaces which simulate the defects of real surfaces. This has been implemented in SIESTA for both modal and FFT-based simulations.

1 Context

The SIESTA simulation program, up to version 4, contained a card called *MIrugo* for the simulation of flatness defects of a mirror surface [5]. The code was based on the model developed in [2], and was intendend for modal simulations only. It has been modified by the author in order to be used in FFT-based simulations as well (available in SIESTA v5r01). This has brought to a re-evaluation of the model, in view of the mirror phase maps now available for the Virgo and Virgo+ mirrors.

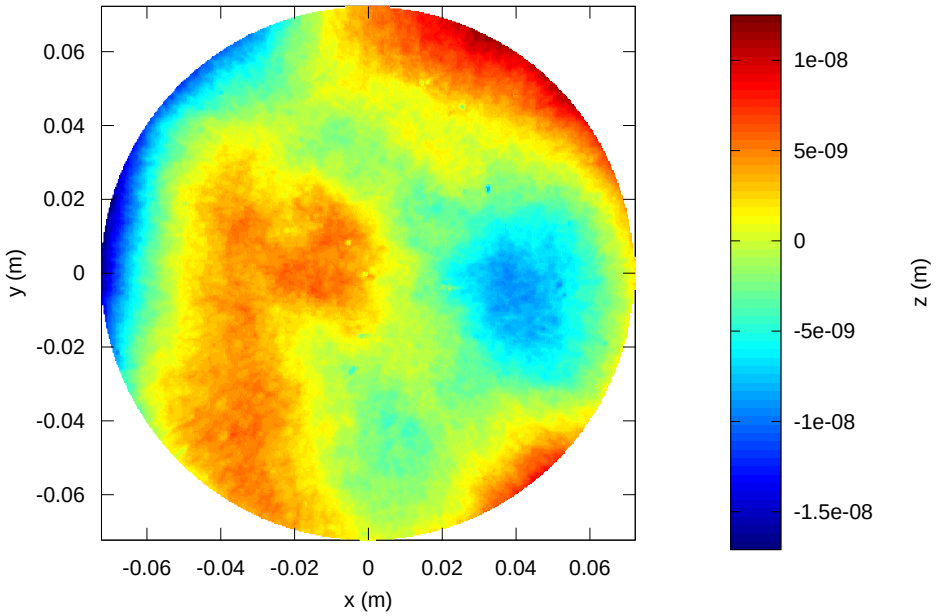

Figure 1: Surface map of the Virgo+ North input mirror (VIM05); the flatness is 4.1 nmRMS.

1.1 Terminology

In order to clarify the terms employed in this note:

micro-roughness is the short-range deviation from the ideal surface (spatial frequencies above $10^3\ \mathrm{m}^{-1}$)

flatness defect is the long-range deviation from the ideal surface (spatial frequencies below $10^3\ \mathrm{m}^{-1}$)

The difference is somewhat more practical than conceptual, being related to the methods and instruments employed to measure the defects. In this note the two terms will be kept distinct; 'flatness' is preferred instead of 'roughness' (as used for instance in the Advanced Ligo specifications) because less ambiguous[1].

Consider a typical situation when running FFT simulations: grid size $\sim 500\,\mathrm{mm}$, number of grid points between 128 and 512. The grid pixel size is therefore $\sim 1\,\mathrm{mm}$ or more. In terms of spatial frequencies, this means covering a band between 1 and $10^3\ \mathrm{m}^{-1}$. We are therefore dealing with surface *flatness*: micro-roughness is too small-scaled for FFT simulations, and will not be taken into account in the following considerations.

2 Modeling flatness defects

Figure 1 shows, as an example, the surface map of the mirror VIM05, currently installed as input test mass in Virgo+ North arm. In order to give a statistical description of such a

[1]In many works about Virgo 'roughness' is used as a generic term for the surface defects, whatever their spatial frequency. SIESTA actually employs the more exotic 'rugosity'.

surface, we follow the method employed in [1, 2, 4]. Briefly, surface defects are described by means of a two-dimensional power spectral density (*PSD*) of the form:

$$S_2(f_x, f_y) = \frac{K_n}{2\pi {f_r}^{n+1}} \tag{1}$$

where f_x, f_y are the spatial frequencies along the x and y axes, $f_r = \sqrt{{f_x}^2 + {f_y}^2}$ is the radial spatial frequency, n is an empirical parameter, and K_n a normalization constant. Since the model assumes the PSD to depend only on the radial frequency f_r, we can conveniently employ the radial 1-D power spectral density:

$$S_1(f_r) = \int_0^{2\pi} S_2(f_r, \phi) f_r \, \mathrm{d}\phi \tag{2}$$

where ϕ is the angular coordinate in the frequency plane. In our case, S_1 simply equals $2\pi f_r S_2$:

$$S_1(f_r) = \frac{K_n}{{f_r}^n} \tag{3}$$

The normalization constant can be determined if the rms flatness is given, knowing that:

$$\sigma^2 = \int_0^{\infty} S_1(f_r) \, \mathrm{d}f_r \tag{4}$$

3 Analysis of Virgo and Virgo+ mirror maps

3.1 Rms flatness

For a given map, the rms flatness is easily computed by directly taking the standard deviation of the map. The value of the rms flatness depends necessarily on the pixel resolution and on the area over which it is computed: the variance being the integral of the PSD (eq. 4), the integration low limit is determined by the diameter of the considered area, and the integration high limit is determined by the spatial resolution. Therefore, the computed rms flatness is larger for larger areas and smaller resolutions.

Table 1 resumes the characteristics of the surface maps for the mirrors of Virgo and Virgo+. The maps have been obtained by measuring the mirror surface with a Fizeau interferometer, and subsequently subtracting piston, tilt, and curvature (Zernike polynomials ${Z_0}^0$, ${Z_1}^{-1}$, ${Z_1}^1$, ${Z_2}^0$).

3.2 Power spectral densities

PSDs have been computed for all the surface maps listed in table 1. For the sake of comparison, all PSDs have been computed over a diameter of 150 mm. The procedure has been coded in Octave and is largely inspired from the Matlab package *MirrorShape* by F. Bondu:

1. if the map is larger than 150 mm, a central circle of diameter 150 mm is cut
2. for the input mirrors, the Zernike polynomials ${Z_0}^0$, ${Z_1}^{-1}$, ${Z_1}^1$ (piston and tilt) are removed

	substrate	*coating*	*map diameter*	*rms flatness*	
Virgo NI	VIM01	c02032	190 mm	2.6 nm	⌀ 60 mm
				3.2 nm	⌀ 150 mm
Virgo WI	VIM02	c02033	190 mm	2.5 nm	⌀ 60 mm
				2.8 nm	⌀ 150 mm
Virgo NE	VEM04	c01077	315 mm	3.8 nm	⌀ 150 mm
				14 nm	⌀ 280 mm
Virgo WE	VEM01	c02017	315 mm	3.4 nm	⌀ 150 mm
				8.9 nm	⌀ 280 mm
Virgo+ NI	VIM05	c09028/1	150 mm	2.2 nm	⌀ 60 mm
				4.1 nm	⌀ 150 mm
Virgo+ WI	VIM06	c09028/2	150 mm	2.9 nm	⌀ 60 mm
				4.1 nm	⌀ 150 mm
Virgo+ NE	VEM10	c09061	315 mm	3.1 nm	⌀ 150 mm
Virgo+ WE	VEM09	c09059	315 mm	5.1 nm	⌀ 150 mm

Table 1: Virgo and Virgo+ mirror maps.

3. for the end mirrors, the Zernike polynomials ${Z_0}^0$, ${Z_1}^{-1}$, ${Z_1}^1$, ${Z_2}^0$ (piston, tilt, and curvature) are removed

4. a Hann window of 150 mm width is applied to the map; the window is normalized in such a way as to conserve the value of the rms flatness

5. the 2-D PSD is computed as the square modulus of the FFT of the windowed map

6. the 1-D PSD is computed by summing, for every radial spatial frequency f_r, all the contributing frequencies f_x, f_y such that ${f_x}^2 + {f_y}^2 = {f_r}^2$

The square root of the PSDs for the eight considered mirror maps are plotted in figures 2–5, where comparisons are made between Virgo mirrors, Virgo+ mirrors, all ITMs, and all ETMs. It has been verified that the integral over all frequencies of the computed PSDs equals the rms flatness.

It can be seen that, in the considered frequency range (approximately between 10 and 1000 m^{-1}), the 1-D PSDs can roughly be represented by a $1/f^n$ law[2].

Figure 6 shows, as an example, the approximation of the PSD of the Virgo+ North input mirror with such a law; it has been found empirically that for the Virgo and Virgo+ mirrors $n \approx 2.3$. This is quite different from the value $1.6 \div 1.8$ found in [4] when characterizing small samples.

4 Generation of random maps

The results of the previous section can be used to generated random maps that reproduce the same distribution of defects (in terms of power spectral density) as the real mirror maps. The parameters to be defined are: the slope n of the PSD; the rms flatness σ, computed over

[2]In [1], the author proposes to model the PSDs with different values of n in different frequency ranges. For the Virgo mirrors, this is surely a better approximation than the one used here; however the aim of the present work is to find a reasonably approximated but more general model, which could be used as well for simulations of future detectors, as Advanced Virgo or Einstein Telescope.

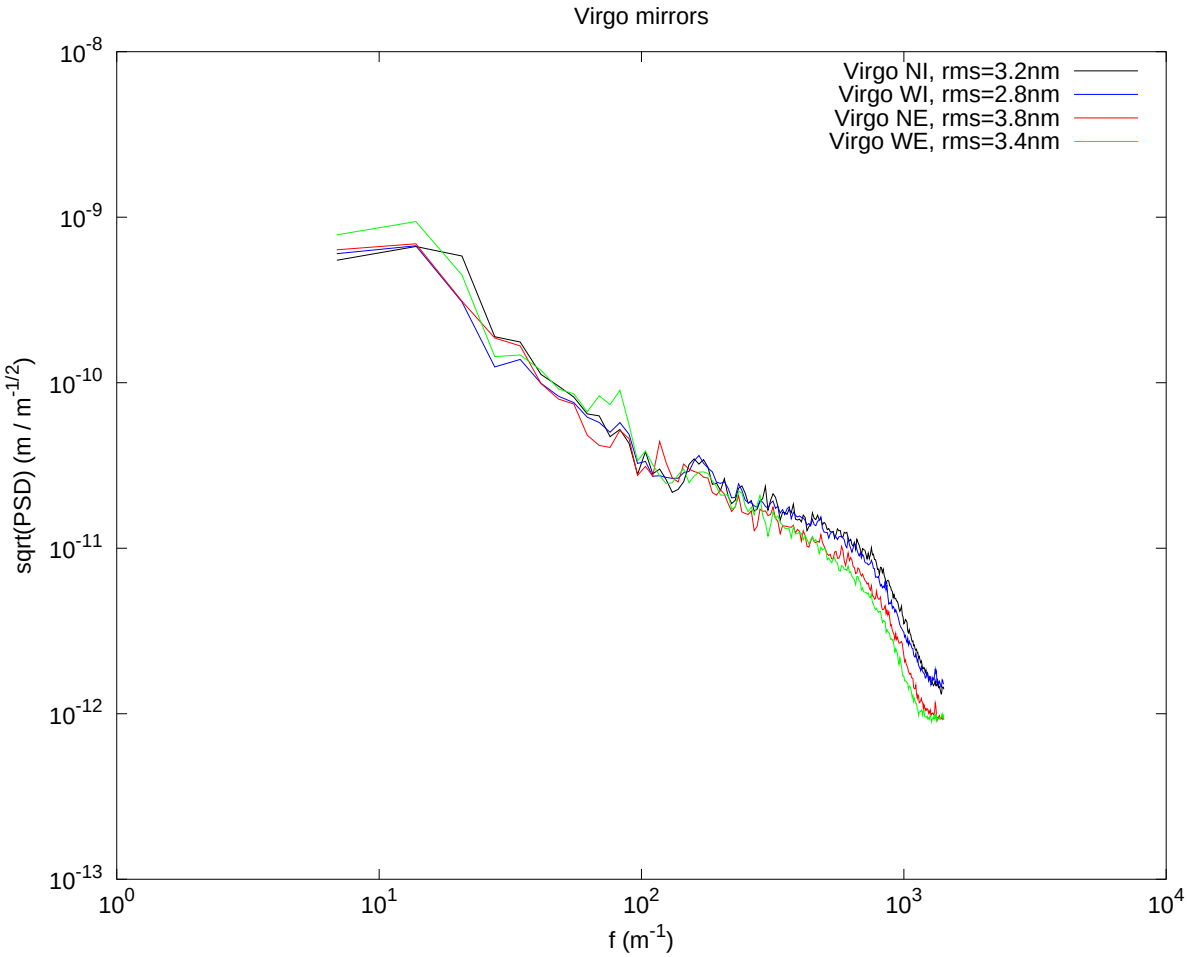

Figure 2: PSDs for the Virgo arm cavity mirrors; only the central area of diameter 150 mm has been used for the computation of the PSD and the rms flatness.

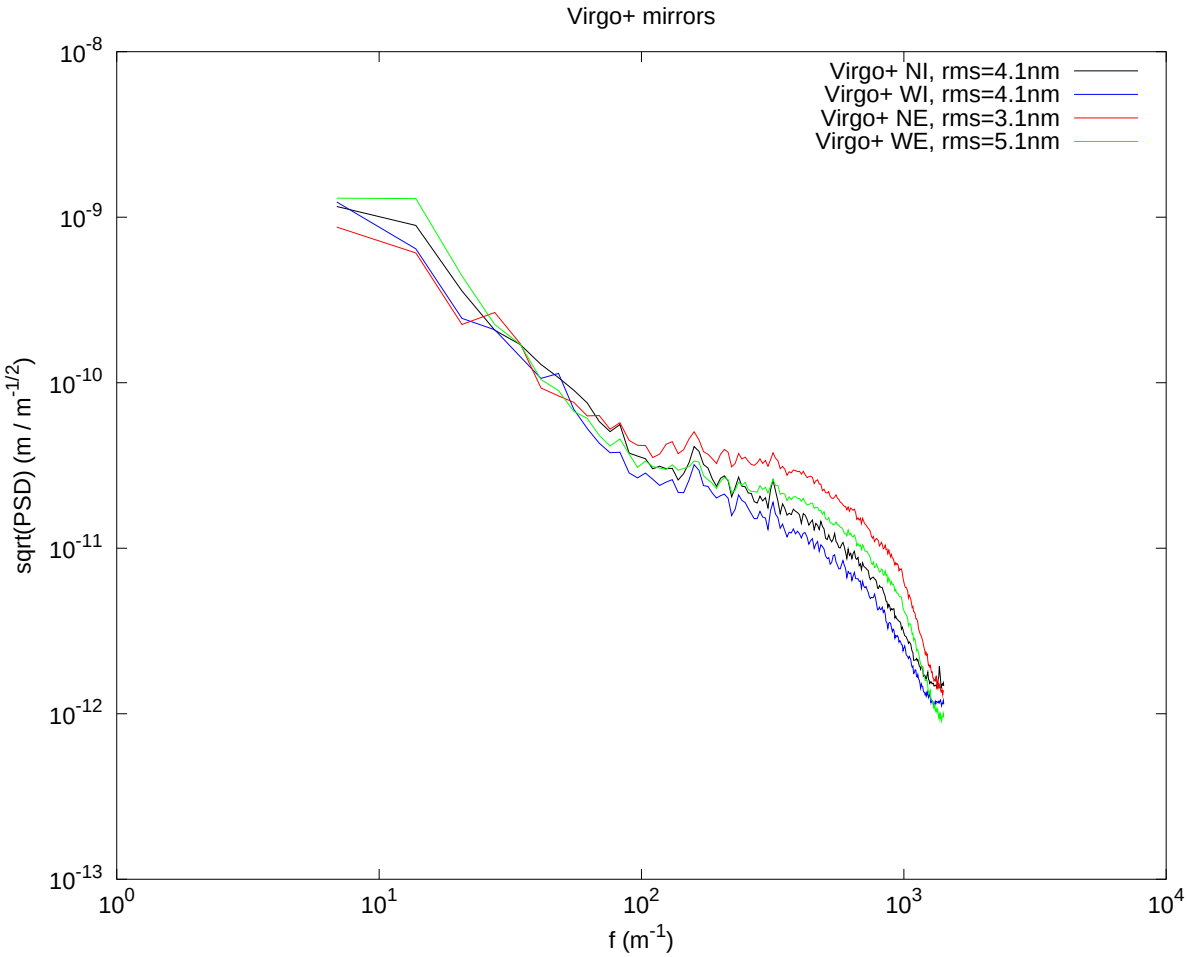

Figure 3: PSDs for the Virgo+ arm cavity mirrors; only the central area of diameter 150 mm has been used for the computation of the PSD and the rms flatness.

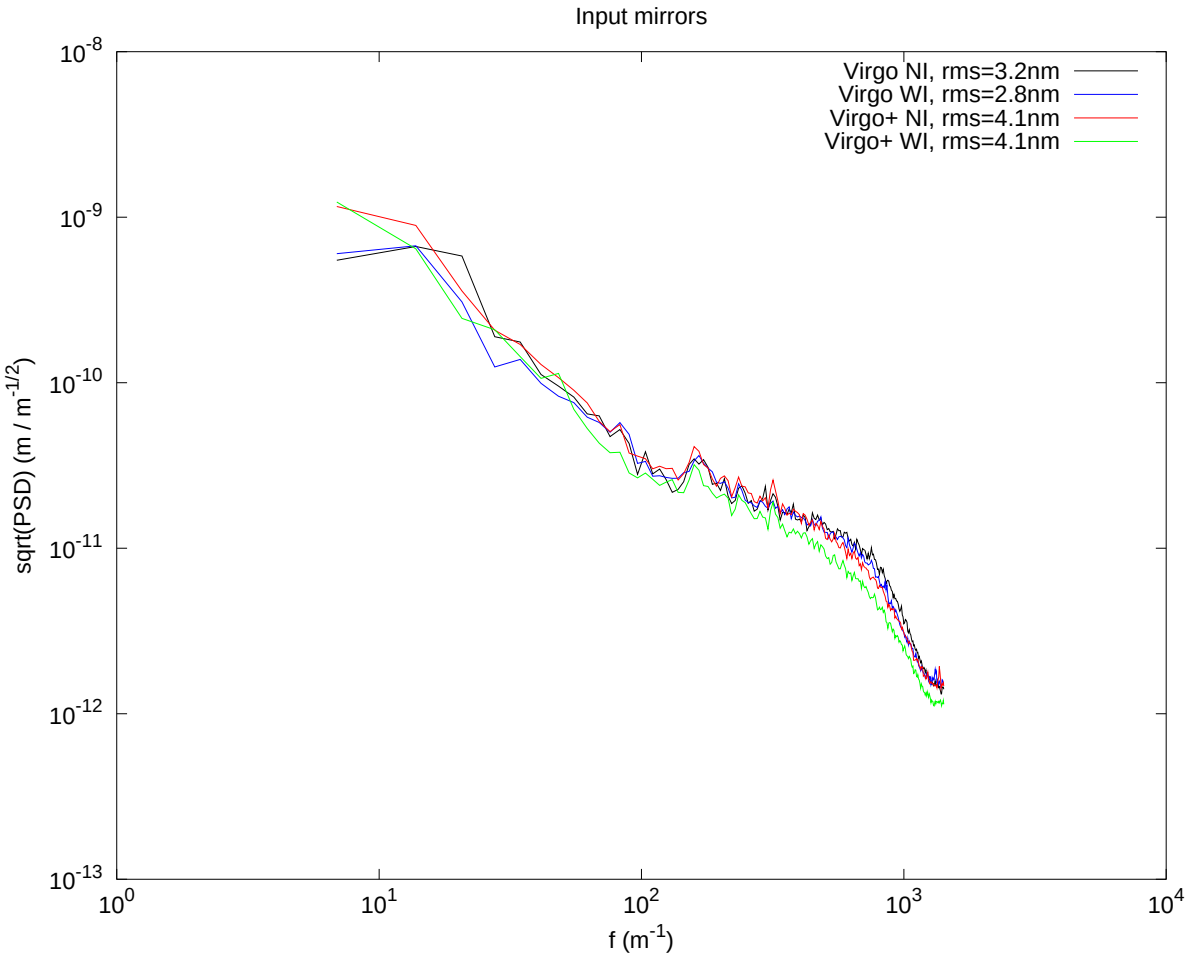

Figure 4: PSDs for the Virgo and Virgo+ ITMs; only the central area of diameter 150 mm has been used for the computation of the PSD and the rms flatness.

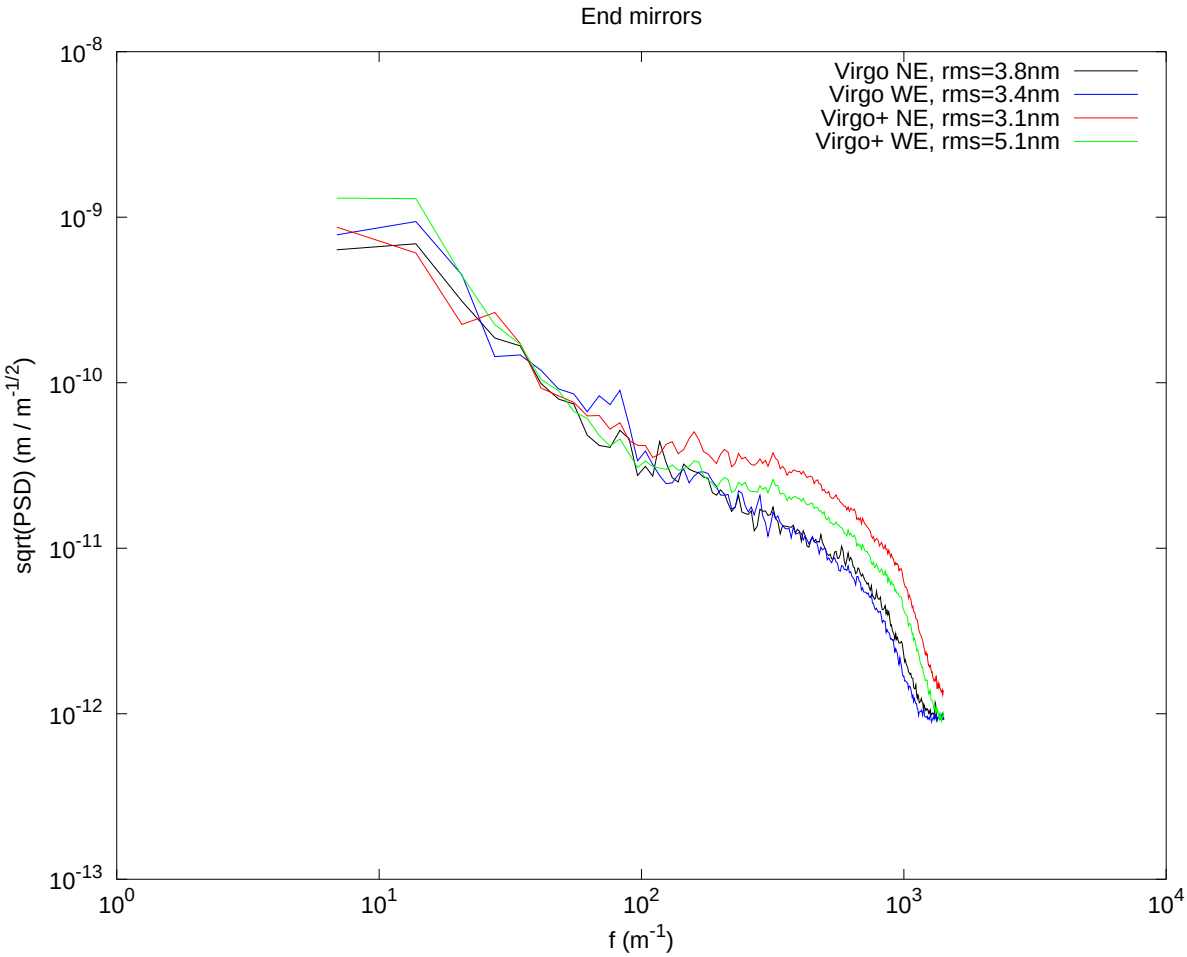

Figure 5: PSDs for the Virgo and Virgo+ ETMs; only the central area of diameter 150 mm has been used for the computation of the PSD and the rms flatness.

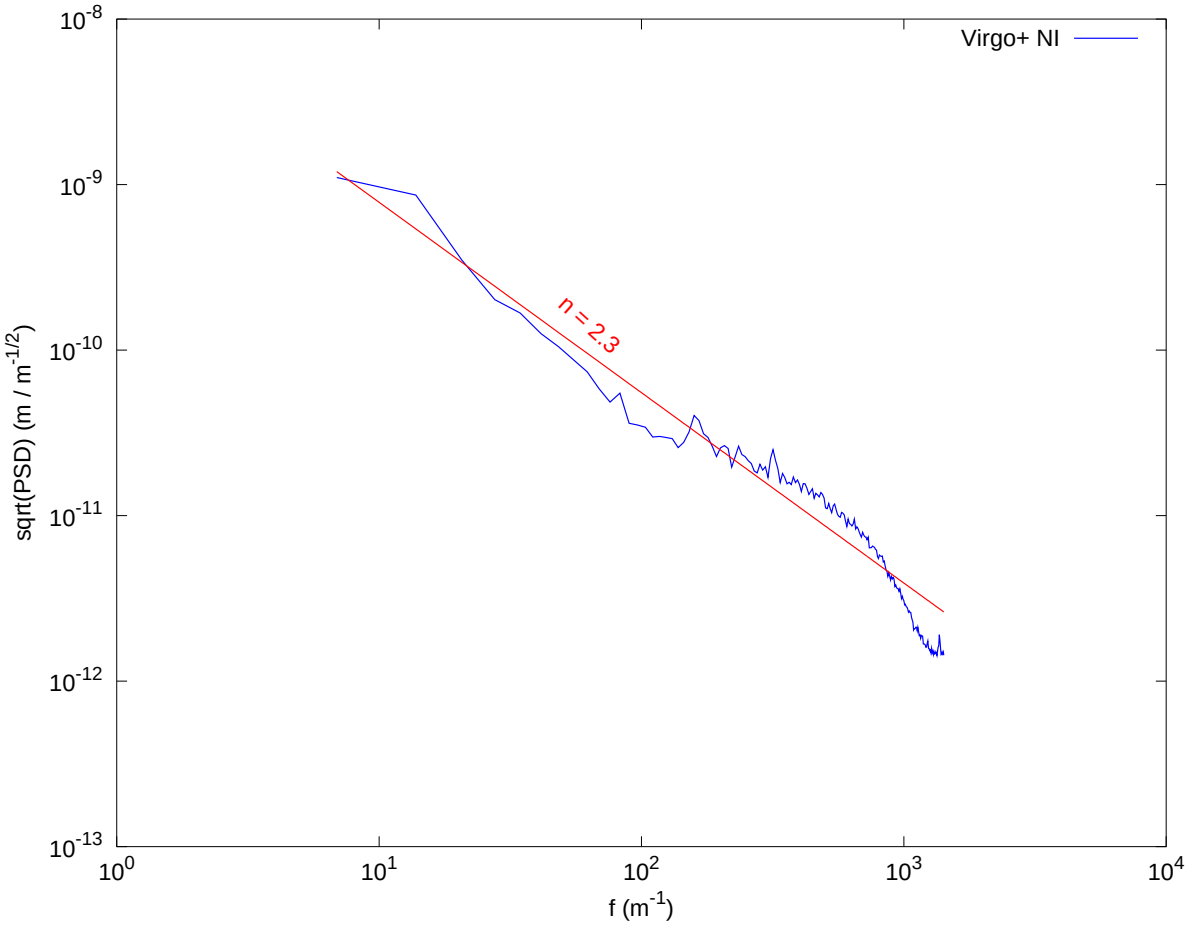

Figure 6: Approximation of the PSD of the Virgo+ North input mirror with a law $\sim f^{-n}$.

a circle of radius R_σ (we recall that the rms flatness depends on the area over which it is defined, see section 3.1). The procedure to generate a random map is the following:

1. A complex matrix M is created in the frequency plane whose modulus equals the square root of the two-dimensional PSD: since $S_2(f_x, f_y) \propto 1/{f_r}^{n+1}$, we set:

$$|M(f_x, f_y)| = \begin{cases} 0 & f_r = 0 \\ {f_r}^{-\frac{n+1}{2}} & f_r > 0 \end{cases}$$

   neglecting for the moment any normalization. $|M|$ represents the modulus of the Fourier transform of the map to be generated.

2. The phase of M is randomly generated, with uniform probability in the interval $[0, 2\pi)$.

3. Having completely defined M (modulus and phase), the surface map is simply computed by inverse Fourier-transforming M.

4. The standard deviation $\tilde{\sigma}$ of the pixels inside the circle of radius R_σ is computed.

5. The map is finally normalized by multiplying for the factor $\sigma/\tilde{\sigma}$, thus assuring that the rms flatness is effectively σ, as defined.

4.1 Comparison between real and generated maps

Random maps have been generated having the same rms flatness as the Virgo and Virgo+ mirrors (see table 1). As an example, figure 7 shows a generated map having the same rms flatness as the Virgo+ North input mirror. The random map has been generated with $n = 2.3$. A comparison of the PSDs of the Virgo+ North input map and the generated one is shown in figure 8.

4.2 Implementation in Siesta

Following the results in the preceding sections, the SIESTA card *MIrugo* has been modified starting from version v5r01[3]. The procedure described in section 4 has been implemented. The user has now to define:

- the radius of the map to generate (which must be less than the grid size in FFT simulations)
- the exponent n of the law $1/f^n$ defining the PSD of the random map
- the rms flatness σ of the random map, and
- the radius R_σ of the area over which such rms is defined.

Further details can be found in the SIESTA User's Guide, version v5r01.

[3]It has been extended to work in FFT simulations as well.

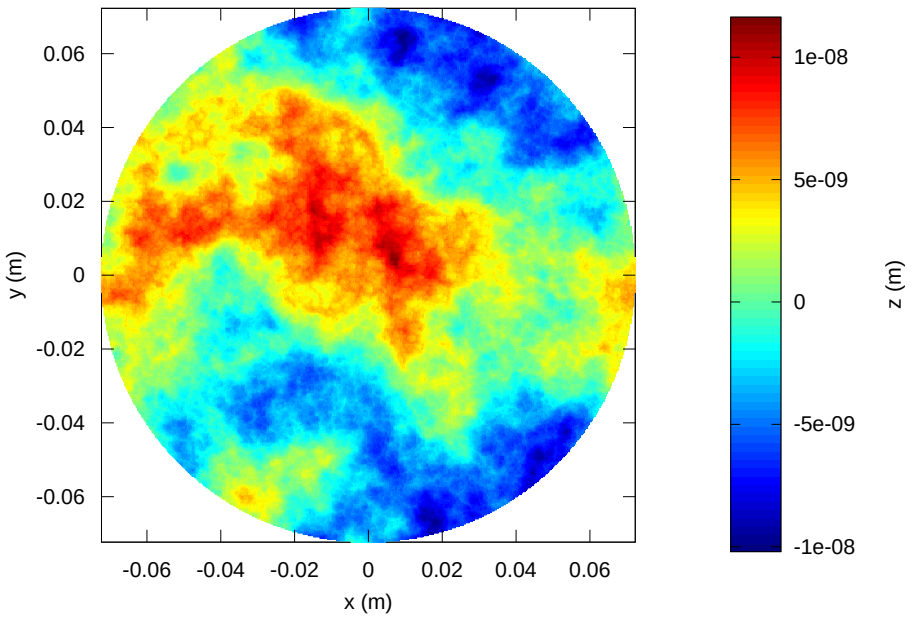

Figure 7: Generated surface map, having the same rms flatness (4.1 nm) of the Virgo+ North input mirror shown in figure 1.

5 Conclusions

The surface defects of the Virgo and Virgo+ mirrors have been characterized by their one-dimensional power spectral density. The PSD can be sufficiently well modelled with a $1/f^n$ law, with $n \approx 2.3$. Such a model is now implemented in SIESTA for the generation of random surface maps.

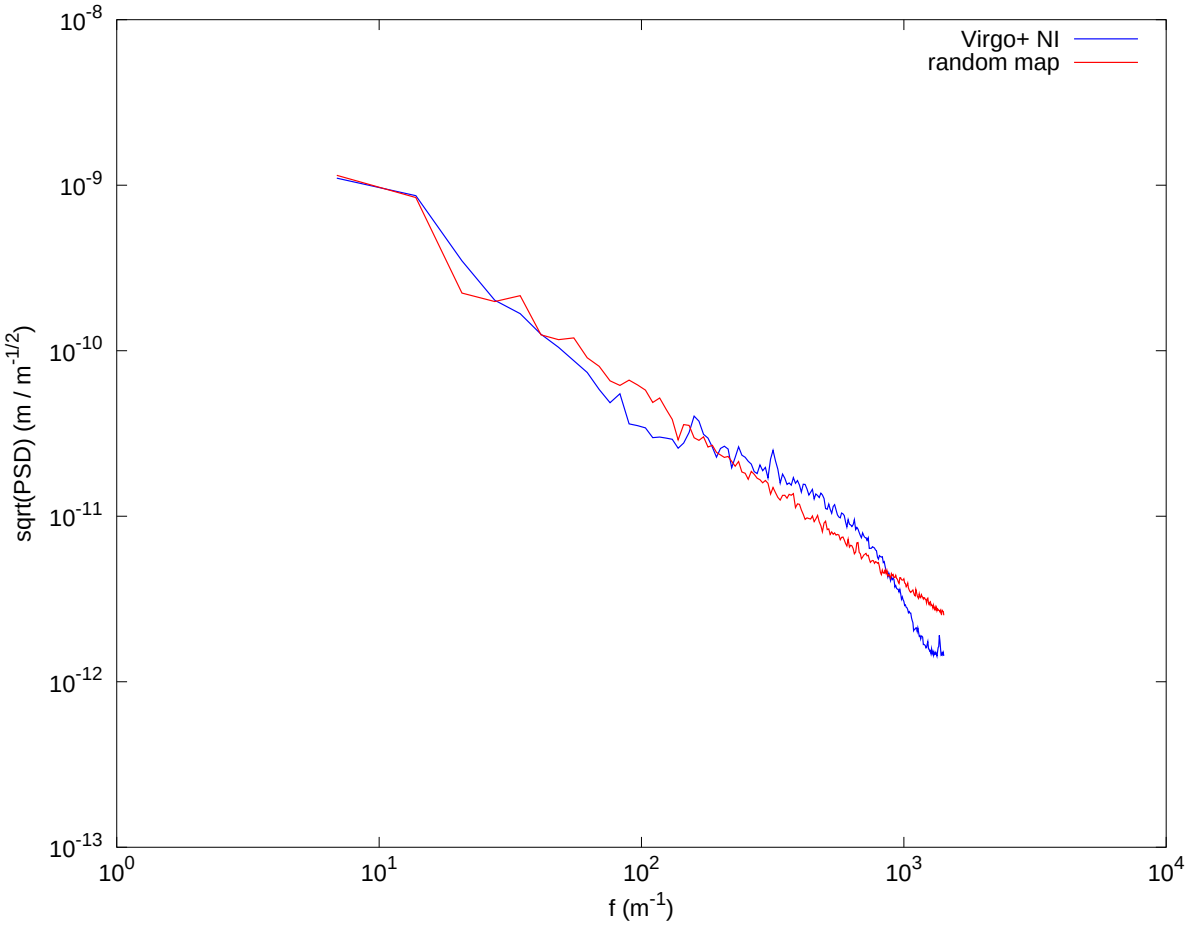

Figure 8: Comparison of the PSDs of the Virgo+ North input mirror and of a generated map with $n = 2.3$. Both maps have the same rms flatness.

Appendix: Power Spectral Density, definitions and usage

Although the definition of the power spectral density (PSD) of a signal in one dimension (for instance in the time domain) is unambiguous, a certain confusion may arise when dealing with two-dimensional functions, as is the case here. This section aims at clarifying the terms employed in the present note.

Stricly speaking, the (two-dimensional) PSD of a two-dimensional function $u(x, y)$ is defined as:

$$S_2(f_x, f_y) = \lim_{A\to\infty} \frac{1}{A}\left|U_A(f_x, f_y)\right|^2 \tag{5}$$

where A is the surface area and $U_A(f_x, f_y)$ is the truncated Fourier transform of $u(x, y)$ over A:

$$U_A(f_x, f_y) = \iint_A u(x, y)e^{-2\pi i(f_x x+f_y y)}\,\mathrm{d}x\,\mathrm{d}y \tag{6}$$

In practice, since the mirror maps have a finite size, the limit $A \to \infty$ is neglected and the PSD is approximated with a two-dimensional periodogram:

$$S_2(f_x, f_y) \approx \frac{1}{A}\left|U_A(f_x, f_y)\right|^2 \tag{7}$$

The 2-D PSD contains the complete spectral information of a mirror map. However, since for a round mirror there are no preferential axes x, y, it seems reasonable to describe the defect distribution by means of a single spatial frequency instead of the pair f_x, f_y. The reader is warned that there are two different and non-equivalent definitions of the one-dimensional PSD which are currently used. The first one, which we may call the *radial* 1-D PSD, is the one used throughout this note (and in SIESTA):

$$S_{1r}(f_r) = \int S_2(f_r, \phi) f_r\,\mathrm{d}\phi \tag{8}$$

where $f_r = \sqrt{{f_x}^2 + {f_y}^2}$ is the radial frequency, and $\phi = \arctan(f_y/f_x)$. The use of S_{1r} is appropriate when the 2-D PSD is radially symmetric, which seems a reasonable assumption for mirror maps. The definition of S_{1r} is such that:

$$\iint S_2(f_r, \phi) f_r\,\mathrm{d}f_r\,\mathrm{d}\phi = \int S_{1r}(f_r)\,\mathrm{d}f_r = \sigma^2 \tag{9}$$

i.e., the integral of S_{1r} over all frequencies gives the variance of the map.

The second defintion is the *profile* 1-D PSD:

$$S_{1x}(f_x) = 4\int S_2(f_x, f_y)\,\mathrm{d}f_y \tag{10}$$

which is none other than the one-sided projection of S_2 on one axis. Again, the integral of S_{1x} over all frequencies gives the variance of the map:

$$\iint S_2(f_x, f_y)\,\mathrm{d}f_x\,\mathrm{d}f_y = \int S_{1x}(f_x)\,\mathrm{d}f_x = \sigma^2 \tag{11}$$

The interest of the profile 1-D PSD is that it is directly related to profile roughness measurements [6, p. 29ff].

The relation between S_{1r} and S_{1x} is not trivial. If S_2 has no rotational symmetry, the two functions are unrelated and there is no way to compute one from the other. However, if the 2-D PSD has rotational symmetry and thus is a function of f_r only, equation (10) can be inverted to give [3]:

$$S_2(f_r) = -\frac{1}{2\pi} \int_{f_r}^{\infty} \frac{\mathrm{d}f_x}{\sqrt{{f_x}^2 - {f_r}^2}} \frac{\mathrm{d}S_{1x}(f_x)}{\mathrm{d}f_x} \tag{12}$$

We get then:

$$\begin{aligned} S_{1r}(f_r) &= 2\pi f_r S_2(f_r) \\ &= -f_r \int_{f_r}^{\infty} \frac{\mathrm{d}f_x}{\sqrt{{f_x}^2 - {f_r}^2}} \frac{\mathrm{d}S_{1x}(f_x)}{\mathrm{d}f_x} \end{aligned} \tag{13}$$

A clear and thorough explanation of the use of PSDs to describe surface defects and of practical issues concerning their computation is given in reference [3].

Acknowledgements

Thanks to François Bondu for his *MirrorShape* code, and for useful clarifications and fruitful suggestions.

References

[1] F. Bondu. Large virtual mirror maps. VIR-0271A-10, 2009.

[2] E. L. Church. Fractal surface finish. *Applied Optics*, 27(8):1518–1526, 1988.

[3] E. L. Church. The optimal estimation of finish parameters. In *Optical Scatter: Applications, Measurement, and Theory*, volume 1530 of *Proc. SPIE*, pages 71–85, 1991.

[4] V. Loriette. Static 1D Virgo'97 simulation by modal decomposition. VIR-NOT-PCI-1380-127, 1995.

[5] F. Marion. *SIESTA User's Guide*, VIR-MAN-LAP-5700-XXX Version 4r01.

[6] J. C. Stover. *Optical Scattering: measurement and analysis*. SPIE, 2nd edition, 1995.